

# Influence of the leprosy drug, dapsone on the model membrane dipalmitoyl phosphatidylethanolamine

Lata Panicker\*

Solid State Physics Division, Bhabha Atomic Research Centre, Mumbai 400085, India

Received 18 January 2006; received in revised form 1 May 2006; accepted 15 May 2006

Available online 22 May 2006

## Abstract

The influence of the sulfone drug, diamino diphenyl sulfone (DDS or dapsone) on the phase transitions and dynamics of the model membrane, dipalmitoyl phosphatidylethanolamine (DPPE)–water/buffer has been studied using DSC and ( $^1\text{H}$  and  $^{31}\text{P}$ ) NMR. These investigations were carried out with DPPE dispersion in both multilamellar vesicular (MLV) and unilamellar vesicular (ULV) forms for DDS/DPPE molar ratio,  $R$ , in the range 0–0.5. DSC results indicate that the mechanism by which DDS interacted with the DPPE membrane is independent of the morphological organization of the lipid bilayer and the solvent (water or buffer) used to form the dispersion. DDS affected both the thermotropic phase transitions and the molecular mobility of the DPPE membrane. Addition of increasing amounts of DDS to the DPPE dispersion, resulted in the lowering of the gel to liquid–crystalline phase transition temperature ( $T_m$ ) hence increased membrane fluidity. At all concentrations, the DDS is located close to the interfacial region of the DPPE bilayer but not in the acyl chain region. The interesting finding with MLV is that the gel phase of DPPE–water/buffer both in presence and absence of DDS, on prolonged equilibration at 25 °C, transforms to a stable crystalline subgel phase(s). The DPPE–water system forms both crystalline subgel  $L_{LC}$  (with transition temperature  $T_{LC} < T_m$ ) and  $L_{HC}$  (with transition temperature  $T_{HC} \geq T_m$ ) phases, while the DPPE–buffer system forms only subgel  $L_{LC}$  phase. The presence of the drug seems to (i) increase the strength of the subgel  $L_{LC}$  phase and (ii) decrease the strength of subgel  $L_{HC}$  (for  $R < 0.5$ ) phase. However, the value of the transition temperatures  $T_{LC}$  and  $T_{HC}$  does not change significantly with increasing drug concentration.

© 2006 Elsevier B.V. All rights reserved.

**Keywords:** DPPE; Differential scanning calorimetry; NMR; Dapsone

## 1. Introduction

Diamino diphenyl sulfone (DDS) or dapsone, a sulfone, is known to be an antimicrobial bacteriostatic [1] and anti-inflammatory drug employed widely for treatment of leprosy [2] and other systemic inflammatory diseases [3,4]. Dapsone as an antibiotic probably acts by a mechanism similar to that of the sulfonamides, inhibiting the synthesis of dihydrofolic acid through competition with para-aminobenzoate for the active site of dihydropteroate synthetase in mycobacteria [5,6]. Therefore, dapsone inhibits the growth of microorganisms that are dependent

on endogenous folic acid synthesis. But dapsone does not affect human being who does not biotransform para-aminobenzoic acid to folic acid. However, only dapsone and not sulfonamides is known to be effective against mycobacterium lepra [7]. The cell wall of mycobacterium lepra contains large amount of unusual lipids, which make the cell walls less permeable [8]. The drug dapsone is lipophilic, as the partition-coefficient ( $\log P$  value) of dapsone in octane–water is +0.97 (lipophilic if  $\log P > 0$ ) [9,10]. Also the solubility of dapsone in water is very low and its dissociation at pH 7.4 is  $< 0.01\%$ . Hence, it is important to understand at a molecular level the mode of action of the drug, DDS with biomembranes and proteins. As a starting step towards understanding DDS–biomembrane interaction, one studies its interactions with the model membranes. Phospholipids one of the important constituents of biomembranes are often used to form the model–membrane system. Phosphatidylethanolamine (PE) and phosphatidylcholine (PC) are major phospholipids found in the biomembrane. In the present study, dispersion of

*Abbreviations:* CM, chain melting; DDS, dapsone; DPPE, dipalmitoyl phosphatidylethanolamine; DSC, differential scanning calorimetric; NMR, nuclear magnetic resonance

\* Tel.: +91 22 25594075; fax: +91 22 25505151.

*E-mail addresses:* [Lata\\_Panicker@yahoo.com](mailto:Lata_Panicker@yahoo.com), [lata@magnum.barc.ernet.in](mailto:lata@magnum.barc.ernet.in).

dipalmitoyl phosphatidylethanolamine (DPPE) in water/buffer is used as the model–membrane system.

The DPPE powder when dispersed in water does not spontaneously form a gel,  $L_{\beta}$  phase at 25 °C [11,12]. The DPPE powder remains in a 3-D ordered lamellar crystalline  $L_C$  phase co-existing with free water, since the DPPE molecules remain unhydrated even in the presence of excess water. This mixture forms gel  $L_{\beta}$  phase, only when heated above the chain-melting transition temperature,  $T_m$  to liquid–crystalline  $L_{\alpha}$  phase [11,12]. The gel  $L_{\beta}$  phase, of saturated PE is known to be metastable and under appropriate conditions (low temperature equilibration), transforms to a stable crystalline subgel  $L_C$  phase [13–17]. The transformation rate being dependent on a number of factors such as thermal history of the sample, the length of the acyl chains and pH of the solvent. This transformation leads to (a) a more ordered packing of the lipids within the bilayer and (b) the expulsion of most of the interlamellar water [16,17]. The strong interactions between the PE headgroup (both intra and inter-bilayer) inhibit the lipid hydration for all temperatures  $T < T_m$ . The strong PE–PE interactions are also responsible for the metastability of the gel  $L_{\beta}$  phase; in model membranes made up of diacyl PEs with saturated chains of length  $C_{10}$ – $C_{16}$  [14,18]. Results of thermal and FTIR studies [14] have led to the conclusion that in the  $L_{\beta}$  phase, the hydrocarbon chains are rotationally disordered although still having an all trans conformation. The  $L_C$  phase is characterized by strong chain–chain and headgroup–headgroup interactions resulting from the highly ordered lipid packing in the bilayer. The DDS–PE interaction would therefore be expected to affect the stability of these phases. This paper describes the effect of the drug, dapsone on the thermal and dynamic properties of DPPE dispersions using DSC and ( $^1\text{H}$  and  $^{31}\text{P}$ ) NMR.

## 2. Materials and methods

### 2.1. Sample preparation

Lipid,  $L$ - $\alpha$ -DPPE, was purchased from Avanti Polar Lipids, Inc., AL, USA, and was used without further purification. The drug, DDS (>99% purity) was obtained from Aldrich Chemical Company, Inc., USA. The buffer of pH 9.3 was prepared using 0.2 M boric acid and 0.05 M borax ( $\text{Na}_2\text{B}_4\text{O}_7 \cdot 10\text{H}_2\text{O}$ ) solution. The model membranes used in this investigation, were in multilamellar vesicular (MLV) and unilamellar vesicular (ULV) form. The method of preparation of the membrane samples in the MLV and ULV forms is the same as that detailed elsewhere [19–21]. The weight fraction of double glass distilled water (with pH 6.5)/buffer to DPPE was 2.5 in MLV. In ULV the lipid concentration [lipid], used were 50 and 25 mM for DSC and NMR experimental work, respectively. The molar ratio,  $R$ , of DDS to DPPE was in the range,  $0 \leq R \leq 0.5$ . From systematic study carried out with DPPE dispersion prepared at different pHs it was found that DPPE formed stable ULV at  $\text{pH} \geq 9.3$  when sonicated for 10 min (forms translucent dispersion). However, at  $\text{pH} < 9.3$  DPPE did not form stable ULV even when sonicated for an hour (the dispersion remains milky indicating presence of MLV also).

Hence, the ULV of DPPE was prepared using buffer pH 9.3 as it formed stable ULV at pH 9.3 [20,21].

For DSC measurements 7–12 mg (for MLV) and 15–18 mg (for ULV) of the samples were hermetically sealed in aluminum pans. To obtain NMR spectra, approximately 1 ml of ULV was taken in a conventional NMR tube. TLC studies on the samples were carried out to check the intactness of the lipid and drug molecules.

### 2.2. Differential scanning calorimeter

Perkin-Elmer DSC-2C instrument was used for thermal measurements of the membrane samples, with an empty aluminum pan as a reference. Temperature calibration of the instrument was done, using cyclohexane and indium at a heating rate of  $10^\circ\text{C min}^{-1}$ . The calibration constants required to calculate the enthalpy values, were obtained using cyclohexane, at heating rates of 10, 5 and  $2.5^\circ\text{C min}^{-1}$ . The chain-melting (CM) transition temperature,  $T_m$ , was obtained by extrapolating the transition peak temperatures (obtained at scanning speed of 10, 5 and  $2.5^\circ\text{C min}^{-1}$ ) to zero scanning speed. The area under the endothermic curve was used to obtain the transition enthalpy,  $\Delta H_m$ . The scans at 5 and  $2.5^\circ\text{C min}^{-1}$  were used for the calculation of CM transition enthalpies. The full width at half maximum,  $\Delta_m$ , used to compare the co-operativity of the CM transitions, was obtained from  $5^\circ\text{C min}^{-1}$  scans. The DSC measurements were carried out for both the MLV and the ULV. Experiments were carried out immediately after the preparation ( $\tau_e \approx 0$ ) of the respective (MLV and ULV) membrane samples. Experiments were repeated again, after equilibrating the samples (a) for 1 day ( $\tau_e \approx 1$  day) at 25 °C and (b) for more than 14 days ( $\tau_e > 14$  days) at 25 °C. For each value of the molar ratio,  $R$ , the experiment was repeated with at least three samples. Data were considered only for those samples in which weight loss was less than 0.2 mg, at the end of the scanning experiments.

### 2.3. Nuclear magnetic resonance (NMR)

$^1\text{H}$  and  $^{31}\text{P}$  NMR spectra were recorded on a Bruker Avance 500 spectrometer equipped with a calibrated temperature control at 500 and 202 MHz, respectively.  $^1\text{H}$  NMR spectra were acquired using a 9000 Hz spectral width into 8 K data points, a 1 s recycle delay, an acquisition time of 0.5 s and a  $\pi/2$  pulse length of 10  $\mu\text{s}$ . The number of acquisitions was 512. The water signal suppression was achieved with pre-saturation of the HDO signal during the relaxation delay of 1 s. The free induction decays (FIDs) were multiplied by a  $90^\circ$  phase shifted sin-bell function before Fourier transformation. For  $^{31}\text{P}$  NMR the broadband proton-decoupled spectra were acquired using a recycle delay of 2 s, spectral width of 60,000 Hz, a  $\pi/2$  pulse length of 17  $\mu\text{s}$  and an acquisition time of 0.67 s. The number of acquisitions was 1024. A line broadening of 10–20 Hz was applied to the FID, before Fourier transformation.

The conventional 5 mm NMR tube containing approximately 1 ml of ULV solution was used to record both  $^1\text{H}$  and  $^{31}\text{P}$  NMR spectra.  $\text{D}_2\text{O}$  and  $\text{H}_3\text{PO}_4$  (85%) were used as external references for  $^1\text{H}$  and  $^{31}\text{P}$  NMR experiments, respectively. The NMR spec-

tra were recorded in the vicinity of the chain-melting transition temperatures of the ULV. At each temperature the samples were equilibrated in the NMR spectrometer for at least 10 min before recording the spectra.

### 3. Results

The DSC heating scans with multilamellar vesicles (MLV) of DPPE in buffer and water, containing increasing concentrations of DDS, obtained at a scan rate of  $5\text{ }^\circ\text{C min}^{-1}$ , and for equilibration time,  $\tau_e \approx 0$  are shown in Fig. 1a and b, respectively. The corresponding molar ratio ( $R$ )-dependence of the thermotropic parameters, the transition temperature,  $T_m$  and the transition enthalpy,  $\Delta H_m$  are given in Figs. 2a and b, and 3a and b, respectively.

The hydrated drug-free DPPE ( $R=0$ ) dispersion in water when heated undergoes a gel ( $L_\beta$ ) to liquid-crystalline ( $L_\alpha$ ) phase transition at  $65.7\text{ }^\circ\text{C}$ . The enthalpy,  $\Delta H_m$ , associated with this transition was  $38.0\text{ kJ mol}^{-1}$ . The values are in agreement with previous reports [22,23]. However, these parameters were found to depend on the pH of the solvent used to form the MLV. Thus, for DPPE–buffer system, the  $T_m$  and  $\Delta H_m$  values were  $64.3\text{ }^\circ\text{C}$  and  $35.6\text{ kJ mol}^{-1}$ , respectively. In both cases incorporation of drug DDS in DPPE bilayer results in shift of the observed transition to lower temperature. The transition enthalpy  $\Delta H_m$  of DPPE–buffer system increased to a small extent in the presence of the drug DDS. However, in DPPE–water system the transition enthalpy  $\Delta H_m$  increases linearly with increasing drug concentration. The presence of drug DDS in both DPPE–water and DPPE–buffer systems did not significantly change the CM transition width.

Thermotropic parameters obtained for samples equilibrated for 1 day ( $\tau_e \approx 1$  day), at  $25\text{ }^\circ\text{C}$  did not change much as compared to their  $\tau_e \approx 0$  values (Figs. 2a and b, and 3a and b). However, interesting changes in their transition behavior were

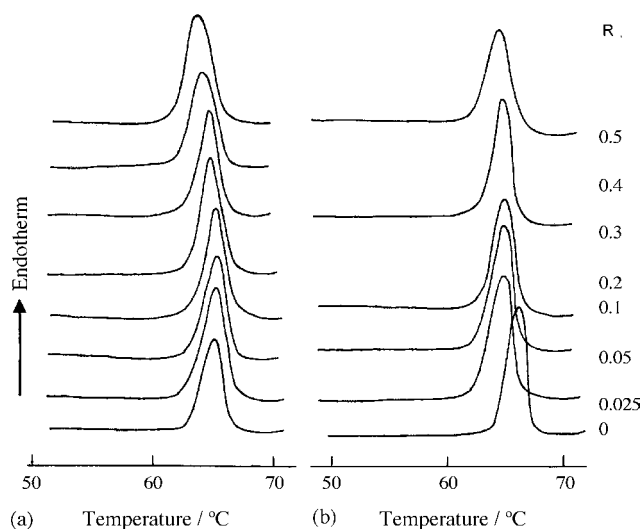


Fig. 1. The DSC heating profiles at  $5\text{ }^\circ\text{C min}^{-1}$  of MLV containing different amount of the drug, DDS and for  $\tau_e \approx 0$ : (a) DPPE–DDS–buffer and (b) DPPE–DDS–water. The molar ratio  $R$ , of DDS to DPPE is indicated on the curve.

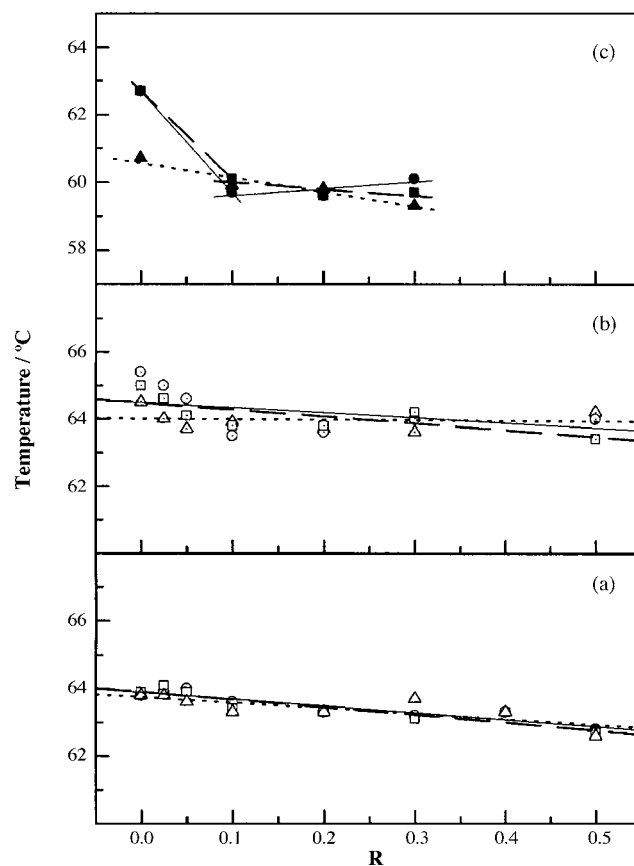


Fig. 2.  $R$ -dependence of transition temperature ( $T_m$ )—(a) DPPE–DDS–buffer: MLV ( $\tau_e \approx 0$  ( $\circ$ ),  $\tau_e \approx 1$  day ( $\square$ ) and  $\tau_e \approx 32$  days ( $\Delta$ )); (b) DPPE–DDS–water: MLV ( $\tau_e \approx 0$  ( $\circ$ ),  $\tau_e \approx 1$  day ( $\square$ ) and  $\tau_e \approx 32$  days ( $\Delta$ )); (c) DPPE–DDS–buffer: ULV ( $\tau_e \approx 0$  ( $\bullet$ ),  $\tau_e \approx 1$  day ( $\blacksquare$ ) and  $\tau_e \approx 15$  days ( $\blacktriangle$ )). The size of the symbol has been chosen in conformity with the error bar.

observed after equilibrating these samples for 32 days ( $\tau_e \approx 32$  days) at  $25\text{ }^\circ\text{C}$ . The first and the second scans recorded with the equilibrated membrane samples are shown in Fig. 4a and b, respectively. The scans for DPPE–buffer and DPPE–water systems are denoted by solid and dash curves, respectively. The  $R$ -dependence of the thermotropic parameters the transition temperatures ( $T_{LC}$ ,  $T_m$  and  $T_{HC}$ ) and the transition enthalpies ( $\Delta H_{LC}$ ,  $\Delta H_m$  and  $\Delta H_{HC}$ ) are given in Table 1. In both cases (DPPE–water/buffer) for drug-free and drug-doped systems the first scan indicated the presence of additional transition(s) due to the formation of subgel phase(s). These additional transition(s) are not seen in the second and the successive scans recorded. The gel phase of drug-free DPPE–water dispersion formed two types of subgel phases (a)  $L_{LC}$  with transition temperature  $T_{LC} < T_m$  and (b)  $L_{HC}$  with transition temperature  $T_{HC} \geq T_m$ . The gel phase of DPPE is known to be metastable and on equilibration gets converted to stable crystalline phase [11,12,24,25]. However, the gel phase of drug-free DPPE–buffer system formed only subgel  $L_{LC}$  phase. In both cases the transition enthalpy,  $\Delta H_{LC}$  ( $\sim 3.0\text{ kJ mol}^{-1}$ ) between the  $L_{LC}$  and  $L_\beta$  or ( $L_\beta + L_{HC}$ ) phases was less than one tenth that of CM transition enthalpy,  $\Delta H_m$ . However, the total transition enthalpy ( $\Delta H_{HC} + \Delta H_m$ ), between the ( $L_\beta + L_{HC}$ ) and  $L_\alpha$  phases was approximately  $102.0\text{ kJ mol}^{-1}$ .

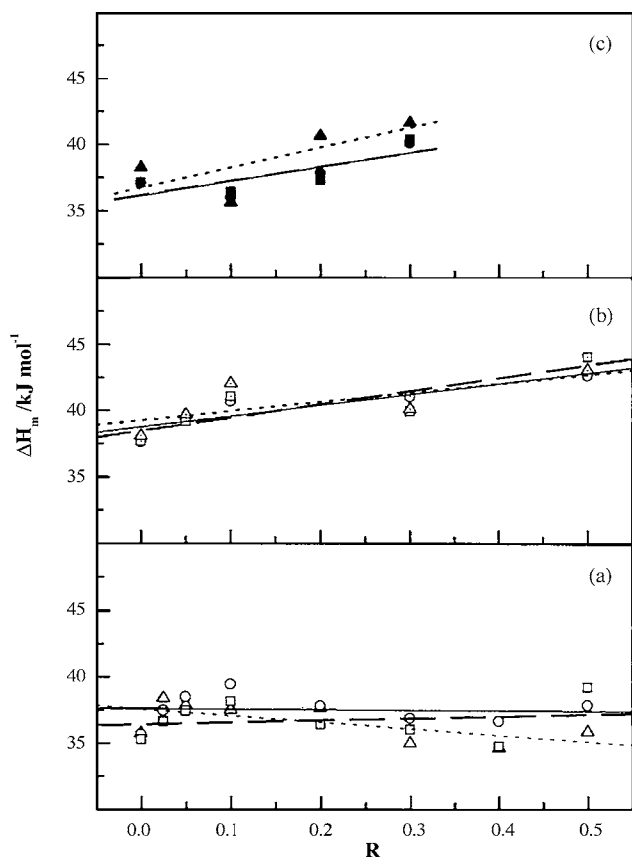


Fig. 3.  $R$ -dependence of transition enthalpy ( $\Delta H_m$ )—(a) DPPE-DDS-buffer: MLV ( $\tau_e \approx 0$  (○),  $\tau_e \approx 1$  day (□) and  $\tau_e \approx 32$  days (Δ)); (b) DPPE-DDS-water: MLV ( $\tau_e \approx 0$  (⊙),  $\tau_e \approx 1$  day (⊠) and  $\tau_e \approx 32$  days (Δ)); (c) DPPE-DDS-buffer: ULV ( $\tau_e \approx 0$  (●),  $\tau_e \approx 1$  day (■) and  $\tau_e \approx 15$  days (▲)). The size of the symbol has been chosen in conformity with the error bar.

The gel phase of DDS-doped DPPE-water when equilibrated also formed more ordered crystalline subgel phases ( $L_{LC}$  and  $L_{HC}$ ). The transition enthalpy,  $\Delta H_{LC}$  and ( $L_{\beta} + L_{HC}$ ) phases increases with increasing drug concentra-

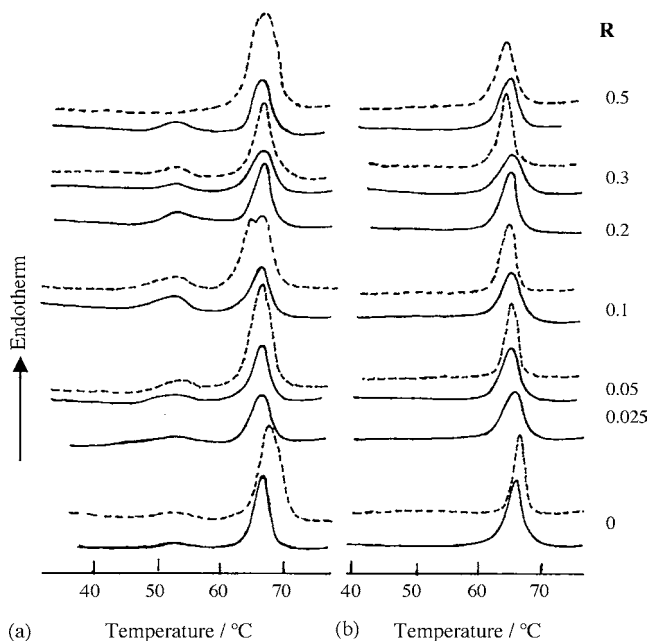


Fig. 4. The first DSC heating scan of MLV with increasing drug concentration obtained after equilibrating it for  $\tau_e \approx 32$  days, is shown on the left side (a) and those on the right side (b) are the second heating scan. The scan speed was  $10^\circ\text{C min}^{-1}$ . The solid curve is for DPPE-buffer system and the dotted curve is for DPPE-water system.

tion for  $R < 0.2$  and decreases with further increase in drug concentration. The total transition enthalpy ( $\Delta H_{HC} + \Delta H_m$ ), between the ( $L_{\beta} + L_{HC}$ ) and  $L_{\alpha}$  phases for  $R < 0.5$  was found to be less than that obtained for drug-free DPPE-water. The  $T_{LC}$  and  $T_{HC}$  values did not change significantly in the presence of DDS. The gel phase of DDS-doped DPPE-buffer system when equilibrated formed only subgel  $L_{LC}$  phase as seen for drug-free DPPE-buffer. The  $T_{LC}$  value did not change significantly in the presence of DDS. The transition enthalpy,  $\Delta H_{LC}$  between the  $L_{LC}$  and  $L_{\beta}$  phases increases with increasing drug

Table 1

Transition temperatures and enthalpies of the first and second heating scan obtained for MLV after equilibrating it at  $25^\circ\text{C}$  for time,  $\tau_e \approx 32$  days

$R_m$	DPPE-DDS-buffer ( $\tau_e \approx 32$ days)				DPPE-DDS-water ( $\tau_e \approx 32$ days)			
	First heating		Second heating		First heating		Second heating	
	$T_{HC/m/LC}$ ( $^\circ\text{C}$ )	$\Delta H_{HC/m/LC}$ (total $\Delta H$ ) ( $\text{kJ mol}^{-1}$ )	$T_m$ ( $^\circ\text{C}$ )	$\Delta H_m$ ( $\text{kJ mol}^{-1}$ )	$T_{HC/m/LC}$ ( $^\circ\text{C}$ )	$\Delta H_{HC/m/LC}$ (total $\Delta H$ ) ( $\text{kJ mol}^{-1}$ )	$T_m$ ( $^\circ\text{C}$ )	$\Delta H_m$ ( $\text{kJ mol}^{-1}$ )
0	52.0 <sub>LC</sub>	3.0 <sub>LC</sub>	–	–	53.6 <sub>LC</sub>	4.0 <sub>LC</sub>	–	–
	66.0 <sub>m</sub>	36.2 <sub>m</sub> (39.2)	65.8	35.7	68.7 <sub>HC and m</sub>	97.8 <sub>HC and m</sub> (101.8)	66.0	43.2
0.025	52.1 <sub>LC</sub>	5.2 <sub>LC</sub>	–	–				
	66.3 <sub>m</sub>	39.3 <sub>m</sub> (44.5)	66.0	40.9				
0.05	52.0 <sub>LC</sub>	6.4 <sub>LC</sub>	–	–	53.3	LC	6.3 <sub>LC</sub>	–
	65.8 <sub>m</sub>	40.4 <sub>m</sub> (46.8)	65.2	40.6	67.7 <sub>HC and m</sub>	75.7 <sub>HC and m</sub> (82.0)	64.8	37.9
0.1	51.5 <sub>LC</sub>	13.5 <sub>LC</sub>	–	–	54.0 <sub>LC</sub>	12.8 <sub>LC</sub>	–	–
	65.4 <sub>m</sub>	44.1 <sub>m</sub> (57.6)	65.7	42.0	66/68 <sub>HC and m</sub>	78.3 <sub>HC and m</sub> (91.1)	65.3	43.5
0.2	52.6 <sub>LC</sub>	3.8 <sub>LC</sub>	–	–				
	66.2 <sub>m</sub>	40.4 <sub>m</sub> (44.2)	66.3	44.9				
0.3	52.3 <sub>LC</sub>	1.4 <sub>LC</sub>	–	–	53 <sub>LC</sub>	4.9 <sub>LC</sub>	–	–
	65.4 <sub>m</sub>	38.2 <sub>m</sub> (39.6)	65.3	35.5	66.5 <sub>HC and m</sub>	58.5 <sub>HC and m</sub> (63.4)	64.7	44.3
0.4	65.4 <sub>m</sub>	37.1 <sub>m</sub>	65.3	36.8				
0.5	52.4 <sub>LC</sub>	4.6 <sub>LC</sub>	–	–	–	–	–	–
	65.3 <sub>m</sub>	38.8 <sub>m</sub> (42.4)	65.0	38.2	67.0 <sub>HC and m</sub>	100.8 <sub>HC and m</sub>	66.0	44.4

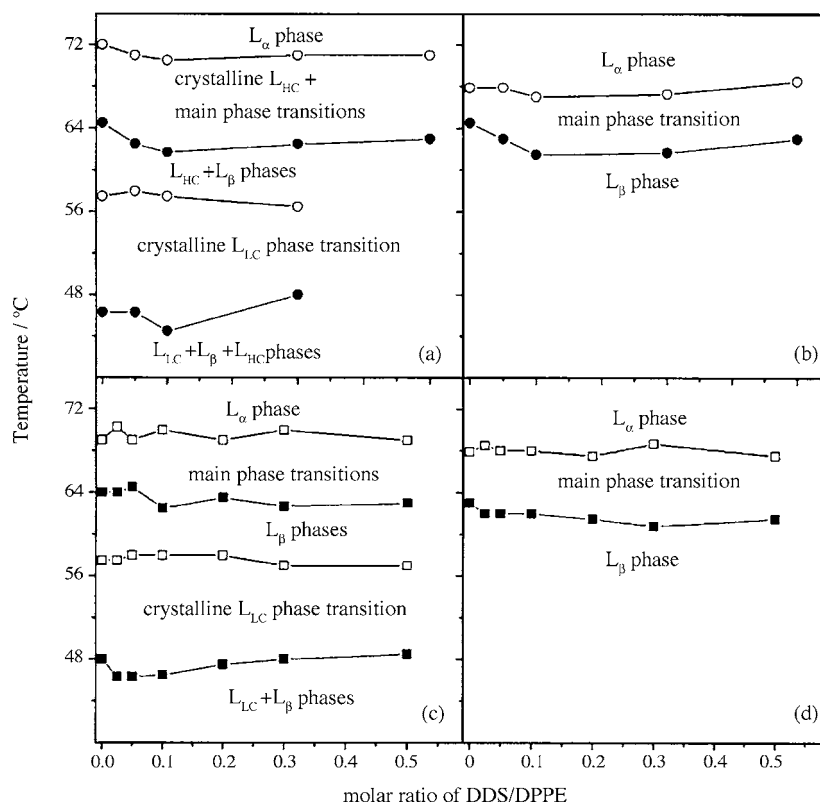


Fig. 5. Thermal phase diagram for prolonged equilibrated samples drawn with data (onset and completion temperature of the transition) from the thermograms given in Fig. 4 a and b. DPPE–DDS–water (● and ○): (a) data from dotted scans of Fig. 4a and (b) data from dotted scans of Fig. 4b; DPPE–DDS–buffer (■ and □): (c) data from solid scans of Fig. 4a and (d) data from solid scans of Fig. 4b. Black symbols and solid lines correspond to the onset temperature of the transitions and open symbols and dotted lines correspond to the completion temperature of the transitions.

concentration for  $R < 0.2$  and with further increase in DDS concentration the  $\Delta H_{LC}$  value got reduced. The successive heating scans (in both cases, DPPE–water/buffer) when compared to  $\tau_e \approx 0$  and  $\tau_e \approx 1$  day scans it was observed that there were no significant changes in the thermotropic parameters (Figs. 2a and b, 3a and b, and 4b). A partial phase diagram was constructed by plotting the onset and completion temperatures of the phase transitions obtained in the first and the second scans with the equilibrated membrane samples (Fig. 4a and b) as a function of drug concentration. The partial phase diagram, which gives information regarding the equilibrium between different phases ( $L_{LC}$ ,  $L_{\beta}$ ,  $L_{HC}$ , and  $L_{\alpha}$ ) in the membranes, obtained with DPPE–DDS–water and DPPE–DDS–buffer systems are shown in Fig. 5a and b, and c and d, respectively. Fig. 5a and c obtained with the onset and completion temperatures of the phase transitions given by dotted and solid scans of Fig. 4a for DPPE–DDS–water and DPPE–DDS–buffer, respectively, shows that these systems consist of mixture of different ( $L_{LC}$ ,  $L_{\beta}$  and  $L_{HC}/L_{LC}$  and  $L_{\beta}$ ) phases. However, the phase diagram (Fig. 5b and d) obtained with the onset and completion temperatures of the phase transitions given by dotted and solid scans of Fig. 4b for DPPE–DDS–water and DPPE–DDS–buffer, respectively, shows that only gel  $L_{\beta}$  exist below the main phase transition.

The DSC measurements were also carried out with unilamellar vesicles (ULV) of DPPE–buffer both in presence and absence of the drug DDS. The DSC profiles, of the ULV obtained at the scan rate of  $5^{\circ}\text{C min}^{-1}$ , for  $\tau_e \approx 0$  and 15 days and for

increasing drug concentrations are shown in Fig. 6. The  $R$ -dependence of the thermotropic parameters is given in Figs 2c and 3c.

The DSC heating thermograms of DPPE dispersion in buffer displayed an endothermic chain-melting transition at a temperature  $62.7^{\circ}\text{C}$  and the enthalpy,  $\Delta H_m$  associated with this transition was  $37.1 \text{ kJ mol}^{-1}$ . The  $T_m$  value obtained was smaller than the corresponding ones for MLV probably due to reduced headgroup interaction in the ULV form because of its high degree of curvature. The width of the transition was increased and was nearly two-fold that of MLV probably due to the presence of ULV with different size and/or few lamella(s).

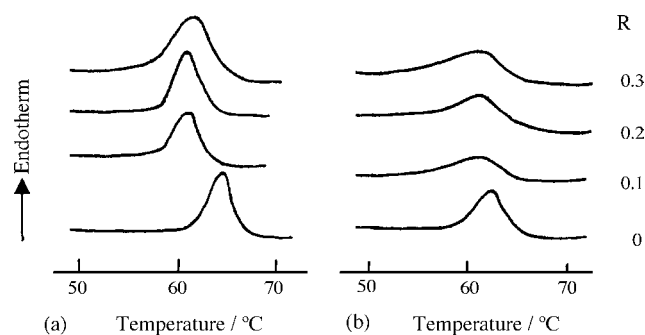


Fig. 6. DSC heating scans at  $5^{\circ}\text{C min}^{-1}$  of ULV: (a) DPPE–DDS,  $\tau_e \approx 0$  and (b) DPPE–DDS,  $\tau_e \approx 15$  days. The molar ratio,  $R$  of drug to lipid is indicated on the curve.

From Figs. 2c, 3c and 6, it is seen that in drug-doped DPPE dispersion the transition temperature is reduced and the enthalpy associated with this transition was increased. This behavior was similar to that observed in MLV. The presence of DDS seems to reduce the effective headgroup–headgroup interaction and increase the acyl chain order.

Thermotropic parameters obtained for samples equilibrated for 1 day ( $\tau_e \approx 1$  day), at 25 °C, did not change much as compared to their  $\tau_e \approx 0$  values (Figs. 2c and 3c.). Prolonged equilibration (Fig. 6 ( $\tau_e \approx 15$  days)) resulted in increased transition width for both drug-free and drug-doped DPPE dispersion, which could most probably be due to the formation of multilayer vesicles with different sizes. The ULV is known to be unstable and fuse to form multilamellar vesicles [26]. The  $T_m$  value was reduced for drug-free DPPE dispersion as compared to its value for  $\tau_e \approx 0$ . However, DDS-doped DPPE dispersion did not show significant change in the  $T_m$  value. The transition enthalpy  $\Delta H_m$  increased on equilibration.

$^1\text{H}$  NMR experiments were carried out with DDS-free and DDS-doped ULV of DPPE. The  $^1\text{H}$  NMR spectra of DPPE molecules in DPPE–buffer and DPPE–DDS–buffer ( $R = 0.2$ ) for various temperatures in the vicinity of  $T_m$  are shown in Fig. 7a and b, respectively. Various proton resonances in the spectra can be identified with the assignments given in inset of Fig. 7. On comparison of DDS-free and DDS-doped DPPE spectra it is seen that in both the cases the chain resonances (1) and (2) were broad and unresolved at temperature less than  $T_m$ . They began to get resolved and became sharper as the temperature approaches  $T_m$ . This sharp increase in chain proton resonance upon phase transition is indicative of more mobility for the concerned proton due to increased chain disorder. Even though the  $T_m$  of DPPE dispersion was affected by the presence of DDS. No significant change was observed in the chemical shifts of the

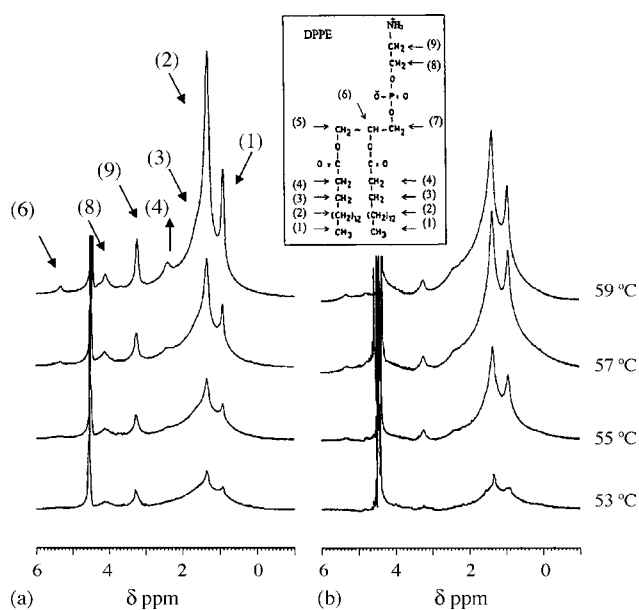


Fig. 7.  $^1\text{H}$  NMR spectra of: (a) DPPE ( $R = 0$ ) and (b) DPPE–DDS ( $R = 0.2$ ) in the vicinity of  $T_m$ . Assignments for the various groups of DPPE are given in the inset. [DPPE] = 25 mM.

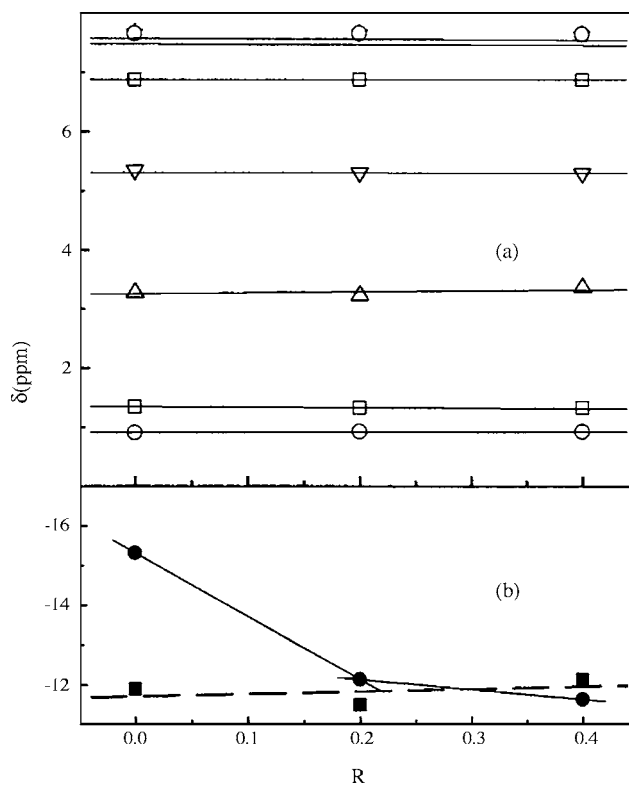


Fig. 8. Change in chemical shifts ( $\delta_{\text{ppm}}$ ) of: (a) DPPE and DDS  $^1\text{H}$  NMR resonances as a function of  $R$  (for  $T < T_m$ ) and (b)  $^{31}\text{P}$  NMR resonances of ULV as a function of  $R$  (for  $T < T_m$  (●) and  $T > T_m$  (■)).

various lipidic resonances. This is clearly seen from the plot of chemical shift ( $\delta_{\text{ppm}}$ ) of the lipidic resonances as a function of  $R$  shown in Fig. 8a for  $T > T_m$  (similar behavior was observed for  $T < T_m$ ). However, the resonances of the various lipidic protons were considerably broadened in DDS-doped DPPE dispersion. The resonances labeled (8) and (3) were hardly seen due to broadening. These results indicate that the mobility of lipidic protons is reduced in the presence of DDS. This would mean that the chains and the ethanolamine groups become more rigid in the presence of DDS. These results suggest that DDS interacts with the  $-\text{N}^+\text{H}_3$  group and perhaps also the carbonyl group of DPPE, the latter leading to decreased chain mobility.

The  $^1\text{H}$  NMR spectra of the aromatic protons, labeled (11)–(14), from DDS in the aqueous medium, DDS–buffer at various temperatures is shown in Fig. 9a. The labeled DDS molecule is shown in the inset of the figure. The spectra of the aromatic protons of DDS obtained from DPPE–DDS dispersions at various temperatures around  $T_m$  are given in Fig. 9b. On comparing the DDS spectra obtained for DDS–buffer (Fig. 9a) and DPPE–DDS–buffer (Fig. 9b) indicated that the DDS interacted with the DPPE bilayer. The fine structure of the aromatic proton resonances of the drug, for  $T > T_m$  almost disappears as the resonances were considerably broadened in the presence of DPPE. However, for  $T < T_m$  the spectra were similar to that of lipid-free dispersion of DDS–buffer. These data suggest that the drug DDS interacted with the DPPE molecules for  $T > T_m$ . However, the values of the chemical shift of various aromatic protons were not significantly changed in the presence of lipid environment

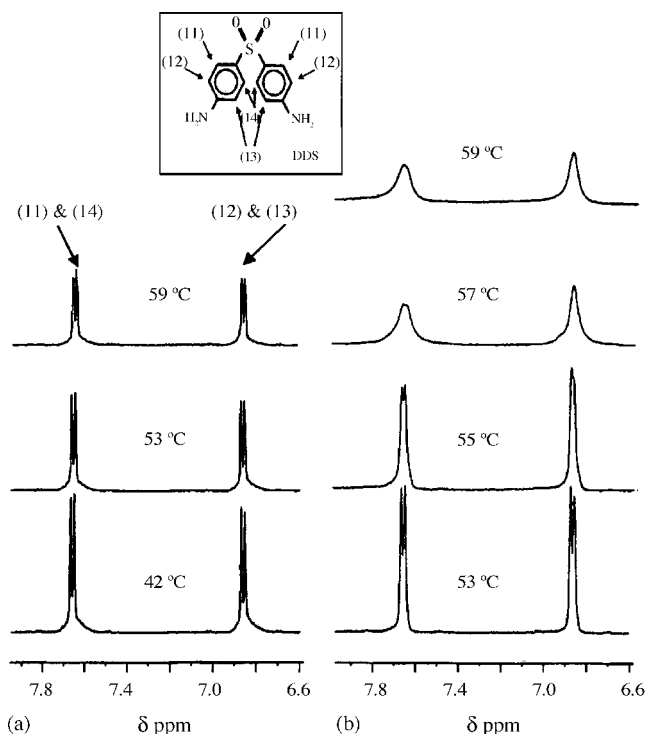


Fig. 9.  $^1\text{H}$  NMR spectra of the aromatic protons of DDS in: (a) DDS–buffer and (b) DPPE–DDS–buffer ( $R=0.2$ ) in the vicinity of  $T_m$ . Inset gives the assignment for DDS. [DPPE] = 25 mM.

(Fig. 8a). The proton resonances corresponding to the  $-\text{NH}_2$  group of DDS was not seen due to exchange processes. The  $^1\text{H}$  NMR results suggest that the aromatic groups of DDS molecules were expected to be located near the lipid glycerol moiety and/or the polar headgroup, with its polar group interacting with (a) the vicinal water, (b) the  $\text{P}=\text{O}$  (DPPE) group or (c) the  $\text{C}=\text{O}$  (lipid) group through hydrogen bonding.

$^{31}\text{P}$  NMR experiments were carried out with DDS-free and DDS-doped unilamellar vesicles of DPPE, to see whether the polar group of DDS interacted with the phosphate group of DPPE. The  $^{31}\text{P}$  NMR spectra from the DDS-free and DDS-doped ULV of DPPE are presented in Fig. 10a and b. The  $^{31}\text{P}$  NMR resonance of DDS-free DPPE dispersion is broad for temperature  $T < T_m$  and becomes sharp for  $T > T_m$ . The broadening of the resonances is due to reduced mobility of the polar headgroup in the gel phase, due to the strong hydrogen bonding interaction between the lipid headgroup. The drug-free DPPE dispersion showed presence of two isotropic signals, which implied presence of two chemically different phosphorous environments. However, the  $^{31}\text{P}$  NMR spectra of DDS-doped DPPE dispersion is sharp for both  $T > T_m$  and  $T < T_m$ . On comparing the  $^{31}\text{P}$  NMR spectra obtained with drug-free and drug-doped DPPE dispersion it shows that the presence of DDS significantly changes the resonance pattern and shifted the ppm values to higher value (clearly seen for  $T < T_m$ ) and is shown in Fig. 8b for  $T < T_m$  and  $T > T_m$ . These results suggest that the polar group of DDS interacted significantly with the polar group of DPPE and hence reduced the  $\text{PE}-\text{PE}$  ( $\text{PO}_4^- - \text{NH}_3^+$ ) headgroup interaction. This interaction seems to leave the phosphorous group

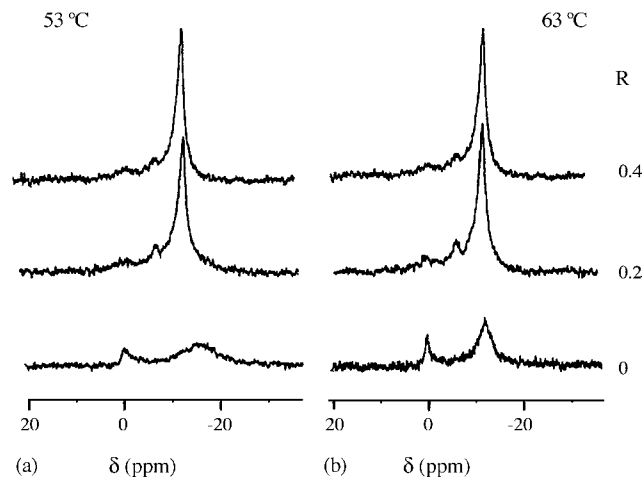


Fig. 10. Proton-decoupled  $^{31}\text{P}$  NMR spectra of DDS-free and DDS-doped DPPE dispersions at temperature: (a)  $T < T_m$  and (b)  $T > T_m$ . The molar ratio,  $R$  of drug to lipid is indicated on the curve. [DPPE] = 25 mM.

free hence increase its mobility and results in a sharp peak even for  $T < T_m$ .

#### 4. Discussion

The DSC results of ULV and MLV indicated that the effect of the drug on the DPPE bilayer was more or less the same in both forms hence independent of the morphological organization of the membrane. The decreased  $T_m$  value and  $^{31}\text{P}$  NMR spectra of the DDS-doped DPPE dispersions suggest that the presence of the drug decreased the headgroup–headgroup interaction of the neighboring DPPE molecules. This is supported by the  $^1\text{H}$  NMR results that the presence of DPPE, lead to a reduction in the mobility of the aromatic protons of DDS. This effect is due to hydrogen bonding and/or electrostatic interactions between the polar groups of DDS and DPPE molecules, which reduce the effective headgroup–headgroup interaction. The drug DDS is lyophilic in nature, hence it is more likely that the polar moiety of the drug get intercalated between the polar groups of the phospholipids. However, the drug is less likely to be present in the acyl chain region of the phospholipid. This is supported by the values of transition enthalpy and the chemical shift (not changed) of the various DPPE proton resonances in the presence of DDS. From DSC results, it was found that the transition enthalpy increased with increasing drug concentration, indicating that the drug increased the acyl chain order. However, in MLV the increase in the acyl chain order was less for DPPE–buffer system when compared to DPPE–water system. The broadening of the proton resonances of DPPE acyl chain in the presence of DDS also indicates that the drug increases the order (rigidity) of the acyl chains. The nature of interaction was found to be similar for the minimum ( $R=0.025$ ) and maximum ( $R=0.5$ ) drug concentration used in this study. Hence, the above results suggest that the drug DDS perturbs the membrane properties which could be of pharmacological importance. Study carried out with DDS-doped dipalmitoyl phosphatidylcholine (DPPC) system showed that DDS interacts with DPPC membrane by affecting both their thermotropic behavior and molecular mobility [30]. The drug

DDS was located close to the interfacial region of the DPPC bilayer. The presence of drug increased the rigidity of the acyl chain similar behavior was observed with DPPE system. However, in the presence of DDS the DPPC membrane reduced the fluidity of the membrane (polar headgroup) by increasing the PC–PC headgroup interaction. This behavior is in contrast to that observed with DPPE wherein presence of DDS increased the membrane fluidity. These differences may be related to stronger PE–PE interaction than PC–PC. Further studies using complementary techniques like fluorescence, Raman spectroscopy and X-ray diffraction will be required to get additional information to support the above findings reported.

Prolonged equilibration ( $\tau_e \approx 32$  days) of drug-free and drug-doped MLV of DPPE (both in water and buffer) resulted in the formation of a crystalline subgel phase(s). The DPPE–water system formed both subgel  $L_{LC}$  and  $L_{HC}$  phase(s) while DPPE–buffer system formed subgel  $L_{LC}$  phase only. This implies that the gel phase of DPPE–buffer is different from the gel phase of DPPE–water. The  $L_{LC}$  and  $L_{HC}$  phases seem to be more ordered than  $L_{\beta}$  phase. Even though the mechanism of interaction of DDS with DPPE dispersions in water and buffer were similar, the effect of equilibrating the membrane at 25 °C resulted in different subgel phases. The strong intra and inter-bilayer hydrogen bonding interaction between the neighboring PE headgroup in DPPE–water system facilitates the subgel  $L_{HC}$  phase formation by sequestering out the inter-bilayer water [18,27]. However, this interaction seems to be reduced when MLV is prepared using DPPE–buffer. Hence in DPPE–buffer system the PE headgroups are available for hydrogen bonding with the neighboring water molecules because of which it may not have formed the subgel  $L_{HC}$  phase. The subgel  $L_{HC}$  phase  $\rightarrow$   $L_{\alpha}$  phase transition was assigned to the simultaneous hydration and acyl chain melting of a poorly hydrated crystalline sample, which gives rise to high change in total transition enthalpy [24]. While the metastable gel  $L_{\beta}$  phase  $\rightarrow$   $L_{\alpha}$  phase transition the enthalpy obtained corresponds only to the melting of the acyl chains. Similar to subgel,  $L_{HC}$  phase in the  $L_{LC}$  phase also the acyl chain order were increased but with less inter-bilayer water sequestering out. The formation of somewhat similar low temperature subgel phase, in aqueous dispersion of dimyristoyl phosphatidylethanolamine (DMPE) has earlier been reported [28,29].

The results clearly indicate that: (i) DDS strongly interacts with DPPE bilayer and creates varied environment for DPPE molecules; (ii) the drug molecules did not become embedded in the acyl chain layer, but get intercalated between the polar groups of the phospholipids; (iii) the drug molecules are responsible for decreased PE–PE headgroup interaction. So the drug DDS behaves like a membrane fluidizer; and (iv) in both systems (DPPE–water/buffer) presence of DDS seems to favor formation of subgel  $L_{LC}$  phase. These results imply that inclusion of DDS in biological membranes probably leads to alteration in membrane function. So, dapsone with high lipophilicity and low ionic

dissociation can interact with cell wall of mycobacterium lepra hence allowing passive transmembrane diffusion to target receptor.

## Acknowledgement

The authors would like to thank Dr. P.S. Paravathanathan for fruitful discussions.

## References

- [1] R.H. Gelber, P. Siu, M. Tsang, V. Richard, S.K. Chehl, L.P. Murray, *Int. J. Lepr. Other Mycobact. Dis.* 63 (1995) 259–264.
- [2] G.L. Mandell, M.A. Sande, *Antimicrobial agents, drugs used in the chemotherapy of tuberculosis and leprosy*, in: Goodman and Gilman's, *The Pharmacological Basis of Therapeutics*, eighth ed., Pergamon, New York, 1990, pp. 1146–1164, (Chapter 49).
- [3] L. Ottonella, P. Dapino, M.C. Scirocco, A. Balbi, M. Bevilacqua, F. Dallegri, *Clin. Sci. Colch.* 88 (1995) 331–336.
- [4] W. Szeremeta, J.E. Dohar, *Int. J. Pediatr. Otorhinolaryngol.* 33 (1995) 75–80.
- [5] I. Chopra, P. Brennan, *Tuberc. Lung Dis.* 78 (1998) 89–98.
- [6] M.D. Coleman, *Br. J. Dermatol.* 129 (1993) 507–513.
- [7] G. Wozel, Dapsone, Georg Thieme, Stuttgart, New York, 1996, pp. 2–26.
- [8] J. Liu, C.E. Barry, G.S. Besra, H. Nikaido, *J. Biol. Chem.* 271 (1996) 29545–29551.
- [9] H.J. Roth, K. Eger, R. Troschutz, *Arzneistoffanalyse: Reaktivitat, Stabilitat, Analytik*, Georg Thieme, Stuttgart, New York, 1985, p. 432.
- [10] T. Scior, G. Raddatz, R. Figueroa, H.J. Roth, H.A. Basswanger, *J. Mol. Model.* 3 (1997) 332–337.
- [11] B.G. Tenchov, L.J. Lis, P.J. Quinn, *Biochim. Biophys. Acta* 942 (1988) 305–331.
- [12] D.J. Vaughan, K.M. Keough, *FEBS Lett.* 47 (1974) 158–161.
- [13] B. Tenchov, R. Koynova, G. Rapp, *Biophys. J.* 80 (2001) 1873–1890.
- [14] R.N.A.H. Lewis, R.N. McElhaney, *Biophys. J.* 64 (1993) 1081–1096.
- [15] M. Kodama, H. Inoue, Y. Tsuchida, *Thermochim. Acta* 266 (1995) 373–384.
- [16] S. Mulukutla, G.G. Shipley, *Biochemistry* 23 (1984) 2514–2519.
- [17] H. Chang, R.M. Epand, *Biochim. Biophys. Acta* 728 (1983) 319–324.
- [18] J.M. Seddon, K. Harlos, D. Marsh, *J. Biol. Chem.* 258 (1983) 3850–3854.
- [19] L. Panicker, S.L. Narasimhan, K.P. Mishra, *Thermochim. Acta* 432 (2005) 41–46.
- [20] L. Panicker, K.P. Mishra, *J. Colloid Interface Sci.* 290 (2005) 250–258.
- [21] L. Panicker, K.P. Mishra, *Biophys. Chem.* 120 (2005) 15–23.
- [22] R. Koynova, M. Caffrey, *Chem. Phys. Lipids* 6 (1994) 1–34.
- [23] J. Stumpel, K. Harlos, H. Eibl, *Biochim. Biophys. Acta* 599 (1980) 464–472.
- [24] H.H. Mantsch, S.C. His, K.W. Butler, D.G. Cameron, *Biochim. Biophys. Acta* 728 (1983) 325–330.
- [25] L. Horniak, E. Kutejova, P. Balgavy, *FEBS Lett.* 224 (1987) 283–286.
- [26] B.Z. Lin, C.C. Yin, H. Hauser, *Biochim. Biophys. Acta* 1147 (1993) 237–244.
- [27] X. Hui, F.A. Stephenson, H.-n. Lin, C.-h. Huang, *Biochim. Biophys. Acta* 943 (1988) 63–75.
- [28] D.A. Wilkinson, J.F. Nagle, *Biochemistry* 23 (1984) 1538–1541.
- [29] M.P. Hentschel, S. Braun, R. Dietrich, L. Trahms, *Mol. Cryst. Liq. Cryst.* 124 (1985) 205–217.
- [30] K.U. Deniz, P.S. Paravathanathan, G. Datta, C.L. Khetrapal, K.V. Ramanathan, N. Suryaprakash, S. Raghotama, *J. Biosci.* 15 (1990) 117–123.